



**HAL**  
open science

## The Acoustics of Liquid Foams

Florence Elias, Jérôme Crassous, Caroline Derec, Benjamin Dollet, Wiebke Drenckhan, Cyprien Gay, Valentin Leroy, Camille Noûs, Juliette Pierre, Arnaud Saint-Jalmes

► **To cite this version:**

Florence Elias, Jérôme Crassous, Caroline Derec, Benjamin Dollet, Wiebke Drenckhan, et al.. The Acoustics of Liquid Foams. *Current Opinion in Colloid & Interface Science*, 2020, 50, pp.101391. 10.1016/j.cocis.2020.101391 . hal-02961728

**HAL Id: hal-02961728**

**<https://hal.science/hal-02961728>**

Submitted on 13 Nov 2020

**HAL** is a multi-disciplinary open access archive for the deposit and dissemination of scientific research documents, whether they are published or not. The documents may come from teaching and research institutions in France or abroad, or from public or private research centers.

L'archive ouverte pluridisciplinaire **HAL**, est destinée au dépôt et à la diffusion de documents scientifiques de niveau recherche, publiés ou non, émanant des établissements d'enseignement et de recherche français ou étrangers, des laboratoires publics ou privés.



# The Acoustics of Liquid Foams

Florence Elias<sup>a</sup>, Jérôme Crassous<sup>b</sup>, Caroline Derec<sup>a</sup>,  
Benjamin Dollet<sup>c</sup>, Wiebke Drenckhan<sup>d</sup>, Cyprien Gay<sup>a</sup>,  
Valentin Leroy<sup>a</sup>, Camille Noûs<sup>e</sup>, Juliette Pierre<sup>f</sup> and  
Arnaud Saint-Jalmes<sup>b</sup>

## Abstract

Beside other transport properties of liquid foams, like the optical or electrical ones, the acoustics of liquid foams reveals a great complexity and non-trivial features. Here we present a review of recent experimental and theoretical results on how a sound wave interacts with either a macroscopic foam sample or with its isolated building blocks (films and Plateau borders). The analysis of the literature allows us to determine what is now well understood, what could be measured in foams by acoustics, and what are the remaining issues and perspectives in this research field.

## Addresses

<sup>a</sup> Université de Paris, CNRS, Laboratoire Matière et Systèmes Complexes MSC - UMR 7057, F-75006 Paris, France

<sup>b</sup> Univ Rennes, CNRS, IPR (Institut de Physique de Rennes) - UMR 6251, F-35000 Rennes, France

<sup>c</sup> Université Grenoble Alpes, CNRS, LIPhy, 38000 Grenoble, France

<sup>d</sup> Institut Charles Sadron, CNRS, 23 Rue Du Loess, 67200 Strasbourg, France

<sup>e</sup> Cogitamus Laboratory, Europe

<sup>f</sup> Sorbonne Université, CNRS, UMR 7190, Institut Jean Le Rond D'Alembert, F-75005 Paris, France

Corresponding authors: Saint-Jalmes, Arnaud ([arnaud.saint-jalmes@univ-rennes1.fr](mailto:arnaud.saint-jalmes@univ-rennes1.fr)); Elias, Florence

Current Opinion in Colloid & Interface Science 2020, 50:101391

This review comes from a themed issue on **Thin Liquid Films and Foams**

Edited by **Raymond Dagastine** and **Sibani Lisa Biswal**

For a complete overview see the [Issue](#) and the [Editorial](#)

<https://doi.org/10.1016/j.cocis.2020.101391>

1359-0294/© 2020 Elsevier Ltd. All rights reserved.

## Keywords

foam acoustics.

## 1. Introduction

Aqueous foams are dispersions of a gas in a liquid. In the liquid phase, chemicals must be added to stabilize the dispersions. Such chemicals are usually low molecular weight surfactants, but they can also be amphiphilic polymers [1] or even particles [2, 3]. Their main role is to adsorb at interfaces, then providing repulsive forces between the bubbles.

Much research has been conducted on aqueous foams in the last two decades [4, 5, 6, 7]. Most of their properties and of their modes of evolution have been studied and reported in dedicated reviews: foaming processes [8], structure [9], the links between stability and physical chemistry [10, 11, 12], or rheology [13, 14].

From most of these studies, two important parameters emerge to characterize a foam: the bubble radius  $R$  and the liquid fraction  $\phi_l$ . Together with the chemical formulation, these two parameters provide the physical characterization of the foam. Their initial values are tightly linked to the process of foaming.

With time, these quantities are modified: the gravitational drainage tends to decrease  $\phi_l$  while coarsening and coalescence increase  $R$ . Moreover, there is a strong coupling between these effects, as both of their dynamics depends on  $R$  and  $\phi_l$ . As a consequence, the macroscopic foam properties evolve with time, and a foam indeed rapidly looks different. To control some foam properties, one needs to set the dynamics of drainage and coarsening, thus implying to monitor  $R$  and  $\phi_l$  within a foam as a function of time, and of the position inside the foam.

Ideally, this has to be done *in-situ* and with non-intrusive methods. In that respect, various approaches have been proposed. A rather simple one is based on the measurement of the electrical properties of aqueous foams. It has been demonstrated that the relative electrical conductivity can be simply related to the liquid fraction [15, 16, 17, 18]. Optical methods are also available, either in the limit of single/low scattering or in the opposite case of multiple scattering [19, 20, 21]. In parallel, more complex methods are also developed, especially to give access to 3D structures, like MRI or X-ray tomography, the latter requiring synchrotron facilities [22, 23].

Still in the spirit of monitoring transport properties, the propagation of a sound wave inside a foam has been often proposed as a possible tool to obtain information on  $R$  or  $\phi_l$ . This was initially motivated by the studies on shock waves absorption in foams [24, 25, 26, 27], which showed that  $\phi_l$  and  $R$  had a strong influence on the acoustical properties of foams.

Our goal here is to draw up a review of the different studies published in the literature; this includes both experiments on 3D foams and on isolated structural elements of foams (single channels and single films), as well as models. We have chosen to emphasize some recent important results, especially those allowing to reconcile apparently inconsistent results. Moreover, the motivation is also to report here the main messages and results arising from the most recent experiments and modelling. We discuss their impact both for practical issues (development of acoustic probes) and more fundamental ones. Lastly, we determine the remaining open questions, and the future routes of research in this field.

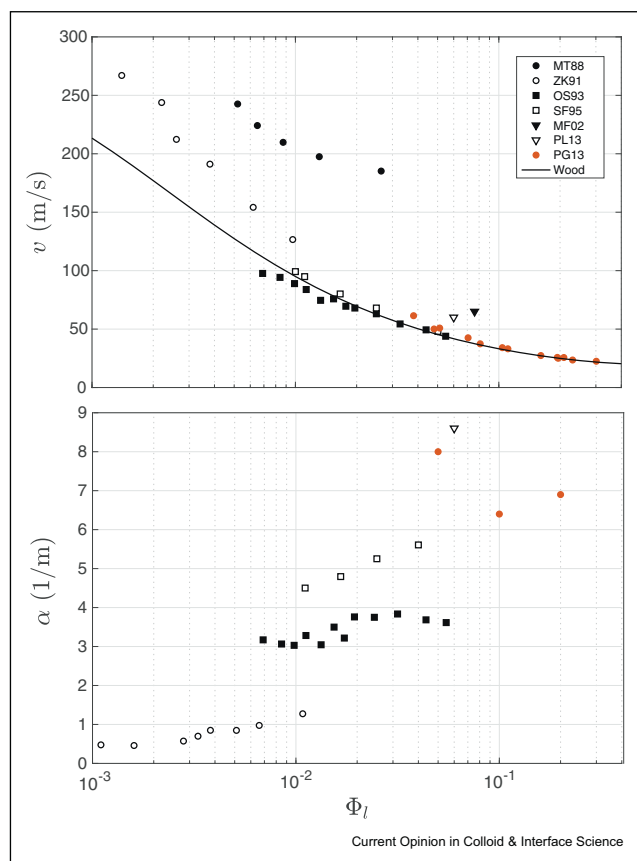
## 2. Acoustic properties

### 2.1. Analysis of the experimental results in the literature

Acoustic experiments on foams generally consist in sending an acoustic wave into a sample of foam, and measuring how this wave propagates. When the acoustic wavelength is larger than the typical size of the heterogeneities, the wave does not resolve the details of the foam, and it propagates like in a homogeneous medium.

The foam is then considered as an effective medium, in which the pressure at position  $x$  and time  $t$  is given by  $p(x, t) = P \exp[-\alpha x] \exp[i\omega(x/v - t)]$  with an amplitude  $P$ , an effective velocity  $v$  and an effective attenuation  $\alpha$ , which depend on the structure and composition of the foam. An important question is thus to relate  $v$  and  $\alpha$  to the different parameters of the foam, such as its liquid fraction  $\phi_l$ , the average radius of the bubbles  $R$ , the type of gas or the nature of the surfactants used to stabilize the foam. Several studies reported measurements of  $v$  and  $\alpha$ , with different techniques, at different wave frequencies, and with different types of foams. We propose in Fig. 1 a summary of seven experimental studies, published between 1988 and 2013, whose characteristics are reported in Tab. 1. It is striking that liquid foams are acoustically very different from the two fluids they are composed of. Their attenuation, in particular, is several orders of magnitude higher than in water ( $2 \times 10^{-9} \text{ m}^{-1}$  at 500 Hz) or in air ( $3 \times 10^{-4} \text{ m}^{-1}$  at 500 Hz). For the velocity, it is very different from the naive expectation of an intermediate value between 1500 m/s (sound velocity in water) and 340 m/s (sound velocity in air): values as low as 25 m/s can be found.

Figure 1



Velocity (top) and attenuation (bottom) as a function of the liquid fraction  $\phi_l$  of the foam for several experimental studies in the literature. Characteristics of the foams and experimental setups used are given in Table 1.

This low value of the speed of sound is actually well predicted by a simple model, proposed by Wood [34]. In this model, sound propagation is sensitive only to the average density  $\rho$  and average compressibility  $\chi$ , and the speed of sound is given by the usual law for monophasic fluids:  $v = 1/\sqrt{\rho\chi}$ . Hence, for a foam Wood's prediction writes

$$v_{\text{Wood}} = \frac{1}{\sqrt{[\phi_l \rho_l + (1 - \phi_l) \rho_g][\phi_l \chi_l + (1 - \phi_l) \chi_g]}} \quad (1)$$

where  $\rho_l$  ( $\rho_g$ ) and  $\chi_l$  ( $\chi_g$ ) are the density and compressibility of the liquid (gas) phase, respectively. The foam thus combines the large compressibility of gas while being relatively dense because of its liquid content, thus explaining the low speed of sound. As the compressibilities and densities of the liquid and gas phases do not vary much from one formulation to the other, this theory predicts that sound speed only depends on the liquid content of the foam,  $\phi_l$ . As obvious in Fig. 1 (upper part), many experimental results are in agreement with this prediction [26, 30, 33, 35, 49, 50], but several publications reported velocities that are larger than Wood's prediction [28, 29, 31, 32]. In their article, Zmashchikov and Kakutkina [29] noted that "This excess can be explained by assuming that not all the liquid participates in the transmission of sound waves." Following the same idea, Kann and Kisilitsyn proposed a "film model" [36], in which only the films in the foam participate to the acoustic movement, leading to a reduced effective density compared to Wood's prediction, and thus a higher velocity. For the results with commercial shaving foams [31, 32] (triangles in Fig. 1), Mujica and Fauve suggested that the high interface elasticity brought by the

Table 1

**Characteristics of the foams (average bubble radius  $R$  and formulation) and experimental setups (frequency  $f$  and size of the container) for the studies whose results are reported in Fig. 1.**

		$R$ ( $\mu\text{m}$ )	$f$ (kHz)	formulation	setup
•	MT88 [28]	1 500	5	air + Expandol	30 cm cubic tank
◦	ZK91 [29]	1 000	0.4	air + Sulfone	15 cm diam. tube
■	OS93 [26]	70-125	0.1	air + unknown	3.5 cm square tube
□	SF95 [30]	100-200	~ 0.5	air + Sulphanole	tube
▼	MF02 [31]	?	5	Gillette	6 cm diam. tube
▽	PL13 [32]	22	0.7	Gillette	2.9 cm diam. tube
•	PG13 [33]	20	~ 0.5	air + C <sub>6</sub> F <sub>14</sub> + SDS	2.9 cm diam. tube

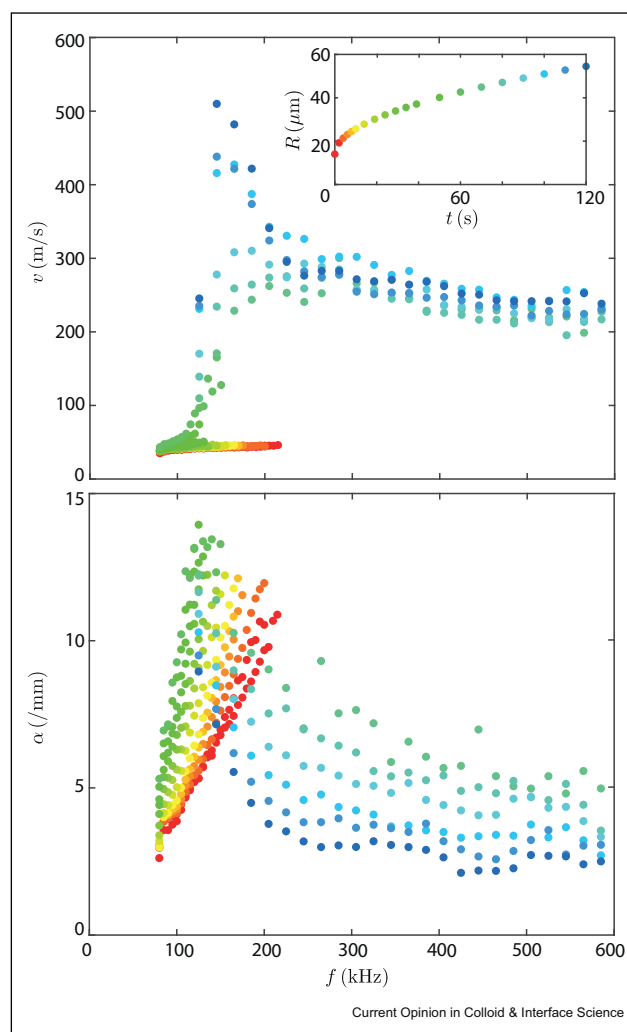
composition of the Gillette foam could be responsible for the deviation from Wood's law.

For the attenuation, the situation is more complicated. As shown in the bottom part of Fig. 1, the general trend is that of an increasing attenuation with liquid fraction, but the data are quite dispersed. It indicates that other parameters play a role. In several studies, the attenuation was found to increase with frequency [31, 26] and with the mean radius of the bubbles [31, 28]. The proposed scaling laws were sometimes compatible with a mechanism of thermal losses [31, 37], but other studies did not find the expected trend in the attenuation when the gas of the foam was changed [25, 38]. Other dissipation mechanisms were proposed, based on Darcy-like flow in the Plateau borders [27] or nonlinear viscous dissipation in the films [36]. However, up to now, there has been no general explanation for sound attenuation in liquid foams. The last experimental results suggest [38, 39] that thermal losses are indeed involved, but other losses need to be considered, including losses due to friction on the wall of the container used for the experiment.

The situation became even more complicated when Ben Salem *et al.* [40] reported evidence of resonance effects in the propagation of ultrasound in foams. When transmission of ultrasound at 40 kHz through a coarsening foam was measured, the amplitude of the signal was first decreasing with time (in agreement with the “ $\alpha$  increases with  $R$ ” law found previously [31, 28]), but then it increased again, indicating a decrease of the attenuation. At the same time, the phase of the transmission was also evolving, showing that the velocity was also strongly, and non-monotonically, affected by the change of the bubbles radius in the foam.

The phenomenon was also observed over a broader range of frequencies, by Pierre *et al.* [41]. Some results of their article are reproduced in Fig. 2. The velocity and attenuation were measured as a function of frequency, in a foam with  $\phi_l = 11\%$  whose bubbles were slowly growing with time (see inset). For the fresh foam (red

Figure 2



Velocity and attenuation as functions of frequency for a liquid foam with  $\phi_l = 11\%$  made from a SDS solution (at concentration 10 g/L) and air saturated with C<sub>6</sub>F<sub>14</sub> for the gaseous phase (raw data from [41]). Colors indicate the median bubble size, which increases with time (see inset in the top figure).

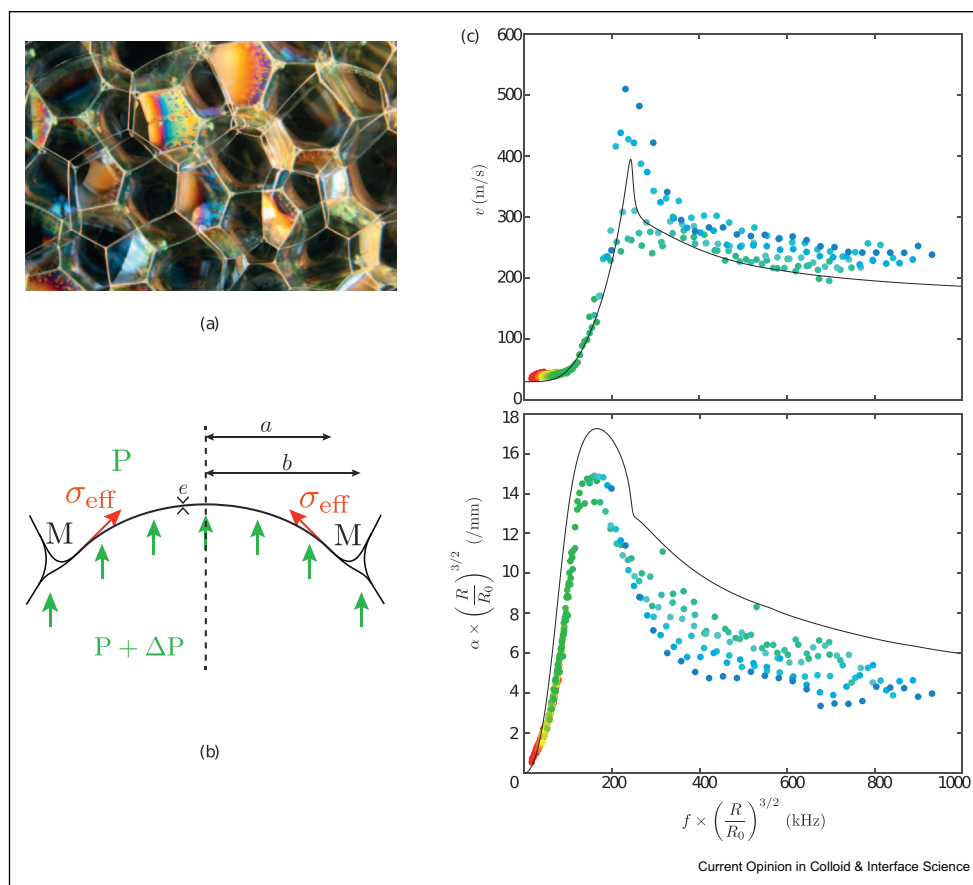
symbols in Fig. 2), the velocity was found to be frequency independent, and in agreement with Wood's law (Eq. 1). But as the size of the bubbles was increasing, the velocity became frequency dependent, exhibiting a peak followed by a plateau at a value of about 200 m/s (see blue symbols). At the same time, the attenuation was found to be first increasing with frequency for small bubbles, and then decreasing for larger bubbles. These experimental results suggested that an acoustic resonance was at play in the foam, with a frequency that depends on the bubble size.

## 2.2. Modeling

In order to model acoustic propagation in foams and rationalize the nontrivial features reported in Sec. 2.1,

Pierre et al. [41] have retained very few items within the foam microstructure. Instead of a full assembly of gas pockets, bounded by thin liquid films attached to thick liquid channels with curvy triangular cross-section (the so-called Plateau borders in the liquid foam jargon, see Fig. 3a), they focused on a single flexible, circular film (surface tension  $\sigma$ , thickness  $e$ , radius  $a$ ) attached to an idealized, circular, undeformable Plateau border (mass  $M$ , radius  $b$ , see Fig. 3b). They modelled its response to a pressure difference  $\Delta P$  oscillating in time with angular frequency  $\omega$ , in particular the channel displacement  $U$  and the film displacement profile  $u(r)$ , where  $r$  is the distance from the center of the film, with  $u(a) = U$  at the junction between the film and the channel. The acceleration of the liquid channel,  $-M\omega^2 U$ , is caused in

Figure 3



(a) Photograph of a low-density liquid foam (less than 1% liquid fraction). Each straight line is located at the junction between three adjacent films and is called a Plateau border, it is actually a water channel with curvy triangular cross-section. Each film is polygonal and bounded by several such water channels. (b) Sketch of the "building blocks" of the model of Pierre et al. [41]: a single liquid film is considered. It is assumed circular rather polygonal in shape, for simplicity. Thus, the system has a cylindrical symmetry around the dashed axis. The film is tethered to a circular water channel with triangular cross-section (the channel is drawn attached to two other films for clarity). From a mechanical point of view, the film is represented by a flexible membrane (here drawn with exaggerated upward deflection) of radius  $a$  and thickness  $e$ . The annular liquid channel (outer radius  $b$ ) is assumed rigid, with mass  $M$ , and the effect of the other two films is ignored. The force exerted by the membrane on the annulus is sketched by the red arrow; its value per unit length of the annular channel is  $\sigma_{\text{eff}}$ . The two bubbles located above and below the membrane are not fully sketched, for simplicity; they have a pressure difference  $\Delta P$  associated to sound propagation, which exerts a surface force on the membrane and on the annulus, sketched by the green arrows. (c) Rescaled data of Fig. 2, superimposed with the model of Pierre et al. [41] using  $\tau = 10 \mu\text{s}$  and  $e = 70 \text{ nm}$  as fitting parameters.

part by the pressure difference applied directly to the channel (with a relevant surface area of order  $\pi(b^2 - a^2)$  in the notations of Fig. 3b) and in part by the relevant component of the tension  $\sigma_{\text{eff}}$  exerted by the film along its perimeter  $2\pi a$  (slope of order  $du/dr$  with respect to the circular channel, evaluated at the junction between the film and the channel):

$$-M\omega^2 U = \pi(b^2 - a^2)\Delta P + 2\pi a\sigma_{\text{eff}}\left.\frac{du}{dr}\right|_{r=a} \quad (2)$$

The factor  $\sigma_{\text{eff}}$  is assumed to be of the form  $\sigma_{\text{eff}} = \sigma(1 - i\omega\tau)$ , which includes not only the film surface tension  $\sigma$  but also a phenomenological time  $\tau$  that reflects out of phase viscous dissipative forces within the channel deformed by changes in the film slope.

Similarly, considering an annular portion of film extending between  $r$  and  $r + dr$  (with surface area  $2\pi r dr$ , thickness  $e$  and liquid specific mass  $\rho_l$ ), its acceleration  $-\omega^2 u(r)$  results both from the applied pressure difference  $\Delta P$  and from the change in film tension slope and perimeter between the inner and outer edges of the annulus:

$$-2\pi\rho_l e r dr \omega^2 u(r) = 2\pi r dr \Delta P + 2\pi\sigma dr \frac{d}{dr}\left(r \frac{du}{dr}\right) \quad (3)$$

At low frequency, this coupled system follows the forcing in a quasisteady manner, the film and the channel vibrating at the same amplitude:  $u(r) = U$ . However, because of the large difference of inertia between the thin film and the thick channel, their response is different as the frequency increases. In particular, in the limit of very large frequencies, the large inertia of the liquid channel prevents it from oscillating, while the film oscillates as if tethered to a fixed frame. An interesting behavior emerges when expanding  $\langle u \rangle$  (defined as the average of  $u$  for  $r \leq a$ ) at frequencies much lower than the fundamental frequency of the film, which is of order  $(\sigma/\rho_l e)^{1/2}/a$  [see Eq. (6) in section 3 for  $q'_f \sim 1/a \gg \rho_g/(\rho_l e)$ ]. In this regime, the ratio of the film acceleration to its driving force quickly decreases and becomes negative as  $\omega$  increases. Moreover, the amplitude of the film quickly dominates that of the liquid channel; hence, the ratio of the system acceleration to the driving force,  $-\omega^2[x\langle u \rangle + (1-x)U]/\pi b^2 \Delta P$  (where  $x = a^2/b^2$  is the surface fraction covered by the film) also decreases and become negative as  $\omega$  increases: the coupled system of the film and liquid channels displays an effective negative mass.

The next step of the model of Pierre et al. [41] was to couple the dynamics of this system to that of the surrounding bubbles, accounting for the gas density and

compressibility in the limit of large sound wavelength compared to the bubble size:  $kR \ll 1$ . The final outcome of this model is a prediction of the sound wavenumber  $k$  such that:  $k^2 = \omega^2[(1 - \phi_l)\chi_g + \phi_l\chi_l](\phi_g\rho_g + \phi_l\rho_l)$ , with an effective liquid fraction  $\phi^l = \phi^l(\phi_l, a, b, \omega)$  given by Eq. (2) in [41] accounting for the coupled dynamics of films and liquid channels. The effective liquid fraction diverges at a resonance frequency  $\omega_0$  defined as:

$$\omega_0^2 = \frac{12N\sigma(1 - \phi_l)}{\rho_l\phi_l x^2 R^3}, \quad (4)$$

where  $N$  is the average number of films per bubble in the direction of propagation of the sound wave. Above this frequency, for a significant range of frequency, the foam displays an effective negative mass and tends to block sound propagation.

This recent model compared favorably with the data (Fig. 3c), and was compatible with all the trends reported in Sec. 2.1. In particular, in the relevant asymptotic limits, it reduces to two models proposed previously. In the limit of low frequency, it gives Wood's model (see Sec. 2.1). This is due to the aforementioned fact that in such a limit  $u = U$ , showing that all liquid elements vibrate at the same amplitude, which justifies the mixture law for the density used by Wood without further justification. In the limit of large frequency, the momentum of the liquid channels can be neglected compared to that of the films and the speed of sound writes

$$v_{\text{HF}} = \frac{1}{\sqrt{\left[\frac{e}{2Rx}\rho_l + (1 - \phi_l)\rho_g\right]\left[\phi_l\chi_l + (1 - \phi_l)\chi_g\right]}}, \quad (5)$$

where  $e$  is the thickness of the films. The regime of the film model proposed by Kann [36] is thus recovered; the main argument of Kann's model is that within a foam, sound propagates as in the gas constituting the bubbles, apart from the additional mass provided by the thin liquid films separating bubbles. This indeed corresponds to the high-frequency limit of the model of Pierre et al. [41].

### 2.3. Sound attenuation

While the models discussed above provide a consistent picture for the speed of sound, the dissipation remains elusive. Kann and Kislitsyn [36] proposed a "sound pumping" mechanism whereby water flow between the films and Plateau borders could be driven by acoustic pressure gradients. Pierre et al. [41] introduced an ad hoc dissipation related to the relative motion of films and liquid channels, through the aforementioned phenomenological parameter  $\tau$ , introduced via the term  $\sigma_{\text{eff}}$  in Eq. (2). However, no clear local transport mechanisms support these ideas, and at this stage of research, dissipation comes mostly as a fitting parameter of the

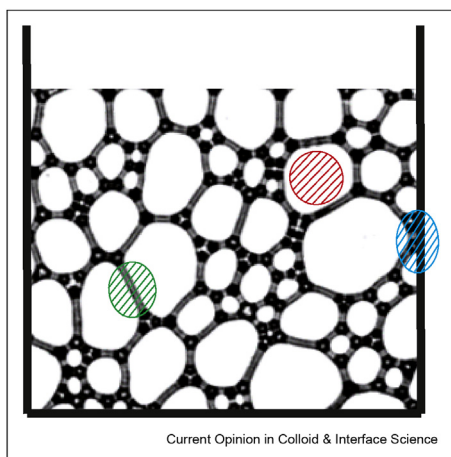
models whose dominant underlying mechanism remains unclear. In this Section, we discuss the possible sources of dissipation.

Fig. 2 shows that acoustic attenuation strongly depends on bubble size and frequency. The toy-model previously exposed catches well the experimental data using a purely ad-hoc dissipation parameter (viscous time  $\tau$ ) which theoretically accounts for the viscous friction between the thin films and the heavy liquid network. However, the way this parameter is introduced is questionable. In particular, it is not obvious that the dissipation remains identical for all frequencies.

Around and beyond the resonance ( $\omega \geq \omega_0$ ), experimental speed of sound and attenuation both strongly change with frequency, and the physical mechanism leading to the dissipation is not easy to identify. However, at low frequency, below the resonance ( $\omega < \omega_0$ ), the velocity is almost constant while, in contrast, the attenuation is widely dispersed with the bubble size and the frequency. Let us focus on this acoustic regime, where the velocity is non dispersive.

Although the nature of the dissipation mechanism is still controversial [25–27, 31, 36, 37, 42, 72], a recent experimental study [38], conducted for various foams made with different gases and with various bubble sizes, using tubes of different diameters, allowed to identify three sources of dissipation, as illustrated in Fig. 4: two intrinsic ones, related to the sound attenuation in the bulk of the foam, and an extrinsic one, related to the boundary conditions (i.e. when the foam is close to a wall).

Figure 4



(a) Sketch of the different dissipation sources which are highlighted by dashed area. The red one indicates the thermal losses. The green zone highlights the viscous losses that may occur in the gas, close to the thin films. The blue zone indicates the viscous friction of the liquid foam on the wall.

The effect of boundary conditions was revealed by the dependence of the attenuation on the diameter of the tube containing the foam. It is explained by the existence of a junction zone between the center of the tube, where the acoustic wave makes the foam move, and its perimeter, where the wall imposes a zero displacement. This zone, over which the foam is sheared, is a source of dissipation. The larger the tube, the smaller this dissipation: this could explain the very low attenuation measured by Zamashchikov & Kakutkina, who used a 15 cm-diameter tube (see ZK91 in Fig. 1) [29]. Note that the existence of this sheared zone was directly observed by optical methods (in the multiple scattering regime) in liquid foams [43, 44, 45].

Removing the contribution of this extrinsic dissipation source, thermal losses are a natural candidate to explain sound attenuation. Their dependence on the gas thermal diffusivity depends on whether the bubble oscillations are isothermal or adiabatic [42], which can complicate data interpretation. However, a recent experimental study [38] reports that thermal losses were not sufficient to explain the level of attenuation, which suggests that a second intrinsic source of loss must be considered. It is found to increase with the square of the bubble size, slightly increase with the liquid fraction and, interestingly, to decrease with the square root of the gas density. It is not compatible with the mechanism of Darcy flow proposed by Goldfarb *et al.* [51, 27]. At this stage, the physical mechanism behind this source of loss remains unclear, it may occur in the gaseous phase close to the thin soap films (Sec. 3).

Finally, it is important to note that all these dissipation mechanisms do not depend on the localized bubble rearrangements continuously occurring within a the liquid foam (such local bubble rearrangements being often named “T1-and T2-events” and due to gas diffusion between adjacent bubbles [4, 5, 6, 7]). In that respect, acoustics is fast enough to probe a “static” foam.

While this discussion concerns low frequencies, below the resonance, attenuation at higher frequency remains a completely open question.

### 3. Vibration at the scale of the elementary building blocks

Soap films and Plateau borders are the subject of deformation waves when exposed to mechanical vibration. Experimentally, they can be studied separately by placing them on a rigid frame. Such an approach makes it possible to describe piece by piece the local elastic, inertial and dissipative forces at play during vibration at the scale of the bubble. Although the full description to move from the bubble scale to the foam scale is not yet complete at this time, we describe in this section the first steps already taken in the literature to understand

the vibration of the liquid skeleton of the foam at the local scale.

Measuring the vibration wave characteristics, namely the wavelength and amplitude, as a function of the excitation frequency and amplitude is a way of determining the force exerted locally on the vibrating element, via the complex wave dispersion relation. Hence, the dispersion relation of capillary waves at the surface of water covered with a surfactant monolayer is a standardized way of measuring the visco-elastic interfacial complex modulus of the monolayer [62, 63, 64]. The monolayer visco-elasticity causes a non-zero

tangential stress in the plane of the interface, which is balanced by a viscous stress that develops in the liquid within a boundary layer of thickness  $\sim \sqrt{\eta_l/\rho_l\omega}$ . The dissipation in the boundary layer represents the main cause for the capillary wave damping.

In a vibrating soap film, however, the soap film thickness ( $\sim 1 \mu\text{m}$ ) is much smaller than the boundary layer in a liquid bulk ( $\sim 10 \mu\text{m}$ ). Hence, viscous dissipation in the film is negligible, and no tangential stress builds up within the film. Investigations of an individual, freely suspended, horizontal soap film (figure 5) have shown, both experimentally and theoretically, that the attenuation of the transverse antisymmetric capillary wave on the soap film originates from the viscous dissipation in the gas phase surrounding the liquid film [59]. A typical image of a horizontal soap film freely suspended on a circular frame and vibrated transversally is shown on Fig. 5a. For a transverse antisymmetric capillary wave propagating in the  $x$  direction on a horizontal soap film, the local vertical film displacement writes  $\zeta(x, t) = \zeta_0 \exp[i(q_f x - \omega t)] = \zeta_0 \exp[i(q'_f x - \omega t)] \times e^{-q''_f x}$ , where  $q'_f$  and  $q''_f$  are respectively the real part and the imaginary part of the complex wave number  $q_f$ . Hence,  $q'_f = 2\pi/\lambda_f$  corresponds to the wavelength  $\lambda_f$ , and  $q''_f$  represents the wave damping, that is the capillary wave attenuation. The complex dispersion relation, that takes into account inertial forces as well as bulk and interfacial viscous and elastic forces, is given by [46, 59]:

$$\frac{\omega^2}{q_f^2} \left( \rho_l e + 2 \frac{\rho_g}{q'_f} \right) = 2\sigma + \mathcal{O}(q'_f e)^2 \varepsilon' \quad (6)$$

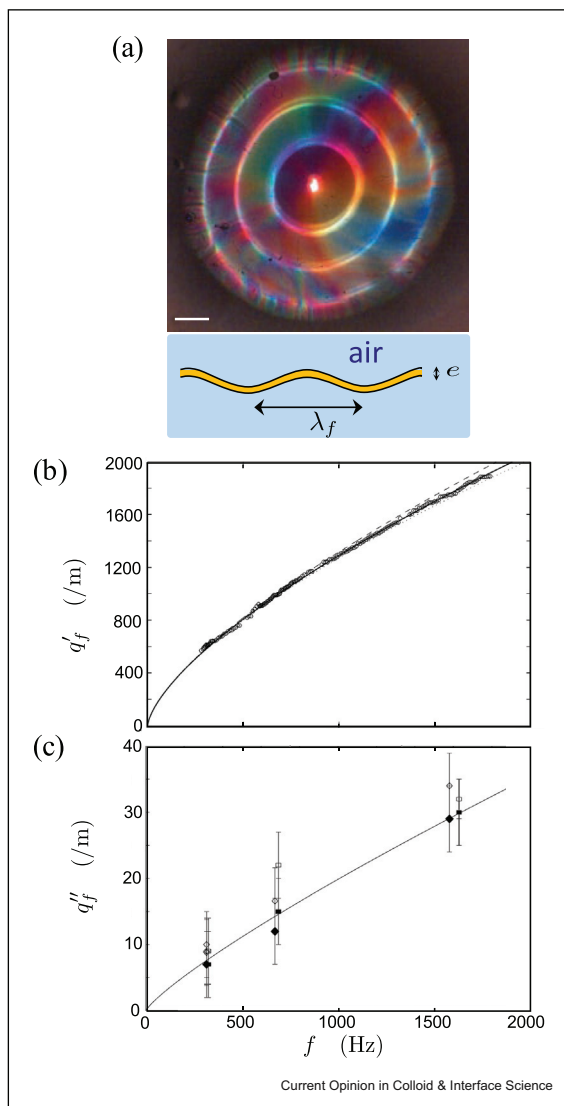
and

$$q''_f = q_f'^2 \frac{\delta_g(\omega)}{3 + q'_f e \rho_L/\rho_g} + \left( \frac{q'_f}{2\sigma} \frac{\rho_l e + 2\rho_g/q'_f}{\rho_l e + 3\rho_g/q'_f} \right) \mathcal{O}(q'_f e)^2 \varepsilon'', \quad (7)$$

where  $\delta_g = \sqrt{\eta_g/(2\rho_g\omega)}$ ,  $\mathcal{O}(q'_f e)^2$  is a term of second order in  $q'_f e$  and  $\varepsilon = \varepsilon' + i\varepsilon''$  is the complex interfacial visco-elastic modulus. Since  $q'_f e$  is typically of the order of  $10^{-3}$ , the term in  $\mathcal{O}(q'_f e)^2 \varepsilon$  is negligible unless  $|\varepsilon|$  is larger than  $1 \text{ N}\cdot\text{m}^{-1}$ . The left hand side of Eq. (6) shows that, as soon as  $q'_f e < \rho_g/\rho_l \sim 10^{-3}$ , which is the case for  $\lambda_f \geq 1 \text{ mm}$ , the gas inertia plays a major role in the response of the soap film to an oscillating forcing. Eq. 7 shows that the capillary wave damping  $q''_f$  is mainly due to the viscous dissipation in the air.

On the other hand, the interfacial visco-elasticity, as well as the viscosity of the liquid phase, play a marginal role in the vibration wavelength  $\lambda_f = 2\pi/q'_f$  and attenuation  $q''_f$ . Fig. 5b and 5c show that the experimental

Figure 5



(a) Vibrating soap film, freely suspended on a horizontal circular frame. The frame diameter is 16 mm and the forcing frequency  $f = 1500 \text{ Hz}$ . The white bar represents 2 mm. Bottom: notations. Real part (b) and imaginary part (c) of the dispersion relation of the antisymmetric wave on the soap film. The solid lines are fits of the experimental data using equations 6 and 7 respectively. (b) and (c) are from ref. [59].

measurements are well described by Eqs. 6 and 7, neglecting second-order terms in  $q'/\rho$ . All those results make the capillary wave propagation on a soap film somewhat different from the propagation of capillary waves on a monolayer.

The modelling of acoustic wave propagation in a foam, however, is based on the coupling between the different sub-structures of the foam, namely the films and the Plateau borders (see Sec. 2.2). Plateau borders are at the line junction between three soap films. Hence they vibrate like the edge of a soap film, loaded with the linear mass of the Plateau border, and submitted to an elastic restoring force due to the capillary traction exerted by the three meeting soap films on the deformed Plateau border [67, 60, 61, 52]. The dispersion relation of vibrating waves on such a Plateau border freely suspended on a prismatic frame has been measured and computed [60]. Its real part results from the interplay between surface tension forces and inertial forces. Three identified inertial contributions add up, coming (i) from the surrounding air, (ii) from the liquid contained in the soap film, and (iii) from the liquid contained in the Plateau border. Since each contribution scales with the frequency as a power law with a different exponent, two asymptotic regimes emerge from the dispersion relation. At low frequency,  $q' \propto \omega^{2/3}$ : the wavelength is not different from that of a freely suspended soap film given by Eq. (6), meaning that the Plateau border vibrates like the passive edge of a liquid membrane. At high frequency, the inertia of the Plateau border comes into play, giving  $q' \propto \omega^2$ . The transition frequency  $\omega_c$  between the two asymptotic regimes depends on the liquid and gas densities, on the surface tension and on the radius  $r$  of the Plateau border:  $\omega_c \propto r^{-3/2}$ . A similar approach, coupling the Plateau border and soap film dynamics, has been used by Seiwert *et al* to successfully describe the oscillations of a circular Plateau border at the junction between a circular horizontal soap film and two other catenary films [61]. The resonant frequency was measured and computed as a function of the liquid and gas densities, the surface tension and on the system geometry, namely the Plateau border cross-section and the soap film dimensions. This work is a first step towards the understanding of the resonant frequency of a foam given by Eq. 4. Further steps require to consider the finite amount of gas enclosed in the bubbles bounded by the coupled system of Plateau border and soap films, as well as bubble-bubble interactions and how these mechanisms change with the bubble size. Indeed, for experimental reasons, the acoustic experiments on isolated soap films and Plateau borders often correspond to large millimetric bubbles, while in most of the acoustic studies on macroscopic foam, bubbles are sub-millimetric.

Understanding the dissipation in such a coupled system remains tricky, both experimentally and theoretically.

On the theoretical aspects, attempts have been made to describe the attenuation of the wave amplitude by considering the bulk or interfacial viscous friction at the transition region between the film and the Plateau border [61, 48]; however, Seiwert *et al* reported that the dissipation does not depend on the viscosity of the liquid phase, which suggests that neither bulk nor interfacial viscous friction are the main contributions to dissipation.

Experimentally, the relaxation time of a transverse wave on the Plateau border [68, 61] has been measured: at low frequency the relaxation time was observed to follow a scaling law compatible with the predicted wave attenuation by viscous friction in the air given by Eq. (7). However, the measured order of magnitude was 5 times larger than the predicted one when considering only the viscous dissipation in the air, which suggests there's still one ingredient missing to understand bubble-scale dissipation. No unified vision exists yet to describe the dissipation at the local scale as a function of the relevant control parameters, namely the geometry of the Plateau borders and the adjacent soap films, the forcing frequency and the forcing amplitude.

In conclusion, we emphasize two main results on the linear vibrating regime of an isolated soap film or an isolated Plateau border: firstly, the major role played by the air viscosity and density, and secondly, the negligible effect of the interfacial viscoelasticity on transverse vibration waves. Those results may directly be exported to the modeling of macroscopic foam acoustic properties. More complex degrees of freedom and couplings, however, remain to be investigated to complete the whole picture, taking into account (i) the dynamics of the vertices at the junction between four Plateau borders [53], and (ii) the compressibility of the air in the bubbles, using an approach similar to the one used to model the vibration of a cubic air bubble in water [55].

At larger amplitude, non-linear effects occur, involving inhomogeneous flow of liquid and air due to the vibration. Although such effects are not at play to describe the interaction between a foam and an acoustic wave of small amplitude presented in section 2, they could be relevant in the propagation of waves of large amplitude in a foam. Several non-linear effects have been identified in vibrated soap films. (i) A self-adaptation effect of the soap film thickness has been reported by Boudaoud *et al*. [47, 69]: due to centrifugal forces, balanced by Marangoni forces, the liquid flows towards the vibration antinodes, which become thicker [47, 69]. (ii) The air, set into net motion by the film vibration via an acoustic streaming effect, induces tangential flow of the liquid inside the films, leading to vortex structures in the plane of the film [46, 65, 69, 70]. (iii) When the soap film is in contact with a reservoir of liquid, the liquid flow within the film may result in the soap film thickening,

increasing the film lifetime [69, 56]. This effect, which also depends on the wave frequency and on the soap film diameter as depicted in reference [56], may in some cases originate from a resonance of the capillary undulation wave on the soap film. (iv) Eventually, a large amplitude may lead to the soap film destabilization and bursting [66, 69].

Performing experiments on a Plateau border isolated on a prismatic vibrated frame, Cohen *et al.* [54] evidenced non-linear inhomogeneities on the Plateau border thickness for large forcing vibration amplitude: the liquid channel splits into two well-separated regions: a thick one and a thin one, whose relative length depends on the vibrating amplitude.

## 4. Key points and outlooks

### 4.1. Control parameters

A first point to address is to check whether all the parameters that affect the acoustic properties of a foam are identified. For macroscopic foam samples, a major result of the recent years was to demonstrate that the frequency and the bubble radius are crucial parameters, together with the liquid fraction (Sec.2). Moreover, these dependencies are understood and have been rationalized within a theoretical framework (Sec.2.2), consistent with the data.

Only in the limit of the lowest frequencies and/or smallest bubble radii does the sound velocity become a function of the liquid fraction only. By contrast, as shown in Fig. 2, it is also in this limit that the attenuation strongly varies with the bubble radii and the frequency.

For frequencies higher than the resonance range (Fig. 3), other structural parameters come into play: it turns out that the sound velocity depends on the film thickness  $\ell$  and on the fraction  $x$  of films on the surface of a bubble (Eq.5), which is directly related to the liquid fraction of the foam [4, 5, 6, 7]. Note that this quantity  $x$  also needs to be taken into account in the prediction of the resonance frequency.

Meanwhile, different experimental results have shown that the gas properties are also important ingredients. Firstly, in the two extreme cases separated by the resonance, the velocity in foams depends on the gas properties (Eq.1, Eq.5). However, note also that, as soon as the liquid fraction is above a few percent, the impact of the gas density vanishes in the low frequency limit. Secondly, as pointed out in Sec.3, the gas properties are important ingredients setting some of the intrinsic dissipation mechanisms.

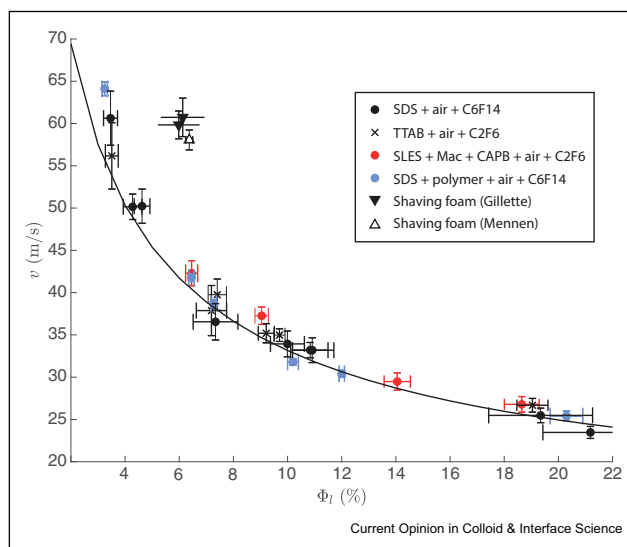
Similarly, from the studies at the intermediate scale of the films and Plateau borders, structural parameters

(size and thickness) and gas properties turn out to be the most important parameters (Sec.3).

Altogether, most results tend to show that the chemical formulation of the foaming solution plays a negligible role. Indeed, the only parameter in relation with the formulation in all the presented equations is the surface tension.

A recent experimental work has been dedicated to these questions [58]. In this work, the formulation of the foaming liquid has been widely tuned (using mixtures of surfactants, co-surfactants, polymers, or proteins), in order to investigate very different bulk and interfacial viscoelasticities. The main conclusion is that the effect of changing the chemical formulation remains small, and is difficult to rationalize. The most significant influence of the foam formulation is found in the approach to the resonance, when the velocity starts to abruptly increase with frequency [58]. Another way to illustrate these issues is to collect sound velocities from different setups and formulations, but selecting only those obtained with experimental conditions below the resonance frequency, and to plot them as a function of the liquid fraction (Fig. 6). According to Wood's formula (Eq.1), the data should then collapse on a single curve. It turns out that the data are indeed consistent with the expected master curve, confirming the small effect of the formulation. Other data (especially those obtained on protein foams, SDS-dodecanol foams or SDS glycerol foams) are also consistent with this picture [58]. However, note that the experiments on commercial shaving foams provide

Figure 6



In the limit of low frequencies (below the resonance), sound velocity for various chemical formulation; only the shaving foams provide a value inconsistent with the others. Line is the Wood's law, Eq. (1).

anomalously high values, when compared to many other systems [31, 32].

One may find surprising that surface viscoelasticity has so little influence on foam acoustics and film vibration, while in the field of ultrasound contrast agent (UCA) microbubbles coated by a viscoelastic monolayer, surface elasticity is known to significantly increase the resonance frequency and surface viscosity is the dominant source of damping [71]. We believe that the key difference lies in the different kinematics of deformation of a spherical bubble in a liquid (for UCAs) *vs.* that of a soap film within a foam. To be specific, let us focus on elastic effects; the discussion is similar for viscous effects. For spherical bubble oscillations, radius variations are directly related to surface dilatation or compression, and it implies that the influence of surface tension on one hand, and of surface elasticity of the other hand, have similar weights; specifically, the resonance frequency is  $\omega_0^2 = \{3\gamma P_0 + [2(3\gamma - 1)\sigma + 4\epsilon'] / R_0\} / (\rho_l R_0^2)$  [71], where  $\gamma$  is the ratio of specific heats,  $P_0$  the atmospheric pressure and  $R_0$  the bubble radius at rest. Hence not only does surface elasticity dominate surface tension as soon as  $\epsilon' > \sigma$ , but also its effect is indeed dramatic for the resonance frequency of microbubbles because its effect becomes of the same order of magnitude as that of gas compressibility (compare  $P_0$  and  $\epsilon'/R_0$  in the above formula). By contrast, the deformation of a vibrating soap film, which is flat at rest, is dominated by variations of curvature, with little surface dilatation or compression, at least when the amplitude of vibration remains small compared to the film wavelength. Hence, a vibrating film develops little viscoelastic surface stress. This shows in Eq. (6) of our review where the tiny weight  $\mathcal{O}(q'e)^2$  multiplies surface elasticity compared to surface tension. Hence only the latter quantity is expected to rule the response of the interface, which explains why interfacial rheology plays so little role in film vibration and foam acoustics.

Finally, the forcing amplitude could also be a control parameter for the acoustic properties of foams, in particular with regard to non-linear properties, which would involve locally observed phenomena such as film and Plateau border thickening [47, 56, 65, 69]. However, to our knowledge, there is currently no work in the literature describing the role of this parameter on the foam acoustic properties.

#### 4.2. Towards acoustic probes for foams ?

Once the parameters on which depend the acoustics of foams have been identified, one can wonder if a new generation of probes based on acoustics could be engineered to monitor the key features of a foam. The most obvious answer is linked to the data shown in Fig. 6. A simple measurement of the speed of sound can actually be used to deduce the liquid fraction. In practice, more

or less complex setups can be found in the literature; however, the measurement has to be done within the relevant conditions i.e. below the resonance frequency. Following Eq. (4), this might become tricky as soon as bubbles have millimetric diameters (requiring frequencies well below 1 kHz).

On the opposite, the other extreme case, above the resonance, could also be used: in that case, an *in situ* measurement of the film thickness  $\ell$  could be foreseen. Experimentally, this requires measurements at high frequencies for small bubbles ( $R < 1$  mm) (Eq. 4), which is precisely the range where such measurements are missing.

The detection of the resonance frequency could be used to measure a bubble size. This method is challenging since it requires to measure the foam acoustic properties over a wide frequency range; however, it would provide an interesting alternative to optical methods in the case of optically opaque foams, since current techniques for bubble size measurement rely on optical techniques.

Still, other approaches can be proposed in terms of acoustic probes for foams: as an example, a recent work suggests that acoustic probes could be interesting to monitor the velocity of a flowing foam [74]. Finally, the recent results tend to show that acoustic approaches are probably not appropriate to monitor interfacial quantities (like interfacial and bulk viscoelastic parameters).

#### 4.3. Remaining questions

In many aspects of foam science, the relevance of experimental studies conducted with isolated structural foam elements (like single films, or Plateau borders, etc...) to shed light on what happens in 3D foams remains an open issue. As a matter of fact, this is also recovered here for acoustic issues. At this stage, it is still difficult to link the results of the experiments on single films and Plateau borders to the ones on foams. Direct transpositions of results obtained on large cm-diameter films to tiny sub-millimeter bubble foams is challenging, as one must take into account all the effects due to the change of lengthscales (for instance, the balance between gravity and capillarity - respectively dominating for large and small sizes). It is also not clear how the imposed vibrations on isolated structures compare to the acoustic forcing within the 3D foam. Lastly, the gas confinement is also different: closed gas bubbles in foam experiments, *versus* open configurations in film experiments. Nevertheless, despite the missing link, we can point out that there appears to be no contradictions between all these experiments: all have evidenced the dynamic coupling between films and Plateau borders, and the rich behavior arising from the differences in shape and mass of these structures.

Therefore, even though the connections to 3D foams are not yet made, it remains probably useful to keep collecting information on what happens at the junction between Plateau borders and films by experiments on these isolated building blocks. In particular, this might help to establish local parameters for the existing global models (see Sec.2.2). In that respect, to make some progress, one needs to fully identify the origins and mechanisms of dissipation, and this probably requires a better description of the liquid flows at local scale. The role of the size distribution and foam polydispersity is also an important issue, which remains to be clarified. Lastly, the origins of results obtained for the shaving foams need to be elucidated (Fig. 6). If a large part of the results tend to show that the chemical formulation plays only a negligible role, the discrepancies found for these shaving foams reveal that some non-trivial behaviors can be detected by acoustic measurements, since explanations based on interfacial and bulk viscoelasticities do not seem to be sufficient (Sec.4.1). It is worth noting that - in terms of acoustics - the shaving foams are providing 'anomalous' behavior, while they are generally considered as model foams (especially, in foam rheology).

#### 4.4. Perspectives

Many developments and axes of research can be foreseen based on the accumulated knowledge, either in terms of applications or in relation with the design of new materials with optimal functionalities. In particular, further progress relies on the development of highly controlled foam structures. For instance, regarding polydispersity issues, the transmission of ultrasound through a single layer of monodisperse bubbles (generated by microfluidics techniques) has been recently investigated [75]. In such a material, it was shown that the sound velocity is only sensitive to the gas phase. Other configurations, like bubble *metascreen* (a single layer of gas inclusions in a soft solid) have also been studied [76, 77]. By tuning the parameters of the metascreen, acoustic superabsorption can be achieved over a broad frequency range. Bubble metascreens can thus be used as ultrathin coatings for turning acoustic reflectors into perfect absorbers [76, 77]. Harazi *et al* have shown that *cubic bubbles* (bubbles pinned to 3D solid frame) can be elementary building blocks for the design of acoustic metamaterials [55]. Other types of acoustic metamaterials have been designed from liquid emulsions which are then solidified by polymerization. Such samples, with controlled spatial gradients of void fraction [78], provide a new class of acoustic gradient-index metasurfaces, with a high acoustic index for broadband ultrasonic three-dimensional wavefront shaping in water. Interestingly, the fabrication is very straightforward and directly based on emulsion technology. Thanks to their acoustic resonance, associated to a strong attenuation peak (Fig. 2 and 3c), and originating in the

foam structure at the bubble (i.e. sub-wavelength) scale, liquid foams fall into the field of acoustic metamaterials, even though their fabrication does not require a precise structural assembly. With the aim of using these properties for the design of soundproofing materials, a future challenge remains to solidifying foams while maintaining their nature as acoustic metamaterials. Connected to the use of polymerized emulsions or foams, an important axis of research is indeed also to investigate the links between liquid and solid foams, and how a better understanding of sound propagation in liquid foams could help to design better solid ones. For instance, Gaulon *et al* studied two types of highly controlled polyurethane foams [73]: classical open-cell ones versus membrane foams, in which thin polyurethane membranes were preserved during solidification. Interestingly, the latter presented better absorption abilities, indicating that membranes could be an asset for sound absorption [73].

New routes of optimization have also been investigated in the field of mitigation of shock wave, evidencing a possible optimization of absorption both by the choice of gas and bubble size [42]. Lastly, researchers are also designing new instruments using an acoustic wave as an original source of solicitation: for instance, new and unconventional rheometry can be proposed at frequencies much higher than what can be done by standard methods [44, 45], as well as instruments for monitoring the velocity of a flowing foam [74].

## 5. Conclusions

The propagation of sound in liquid foams, in terms of velocity and attenuation, turns out to be a rather complex problem, far more complicated than any straightforward predictions considering the foam as an effective medium. This is surprising, since all the complex features reported in the literature deal with wavelengths which are always larger than the bubble sizes.

The complexity arises from the differences in size and mass of the different elementary building blocks of a foam skeleton: non-trivial coupling occurs between the oscillations of the flat large thin films and of the much heavier liquid channels.

Despite this complexity, a clear picture has emerged in the last years: when varying either the frequency or the bubble size, there is a shift between two limits, separated by an intermediate regime which includes a resonance of the film-Plateau border element. Unexpectedly, the resonance regime is associated with an effective negative density. A second major and rather unexpected result is the low dependence of the acoustic properties of a foam on its chemical formulation.

Today, the understanding of how sound propagates into a liquid foam could possibly be used to monitor liquid fraction or film thickness, but only if measured in dedicated experimental conditions of bubble sizes and frequencies. The perspectives of using sound and foams are numerous, especially towards the development of new metamaterials, and relying on more and more control of the foam structures.

As a last general message, the recent progresses in foam acoustics are again a good example that foam science requires interdisciplinary approaches, bringing together different expertises from physics to chemistry, as well as experimental skills and modeling.

### Declaration of competing interest

The authors declare that they have no known competing financial interests or personal relationships that could have appeared to influence the work reported in this paper.

### Acknowledgments

We acknowledge funding support from Agence Nationale de la Recherche in the frame of the SAMOUSSE project (Grant No. ANR-11-BS09-001). We thank all the participants of this project for fruitful discussions.

### References

Papers of particular interest, published within the period of review, have been highlighted as:

- \* of special interest
- \*\* of outstanding interest

1. Monteux C, R C: *Physique* 2014, **15**:775.
2. Tcholakova S, Denkov ND, Lips A: *Phys. Chem. Chem. Phys.* 2008, **10**:1608.
3. Stocco A, Rio E, Binks BP, Langevin D: *Soft Matter* 2011, **7**:1260.
4. R. K. Prud'homme, S. A. Khan, *Foams: Theory, Measurements, and Applications*, Marcel Dekker Inc., New York (1997).
5. D. Weaire and S. Hutzler, *The Physics of Foams* (Oxford University Press, New York, 1999).
6. I. Cantat, S. Cohen-Addad, F. Elias, F. Graner, R. Höhler, O. Pitois, F. Rouyer, A. Saint-Jalmes, *Foams: Structure and Dynamics*, 1st ed., edited by S. J. Cox (Oxford University Press, Oxford, 2013).
7. *Foam Films and Foams: Fundamentals and Applications* 1st Edition. editors: D. Exerowa, G. Gochev, D. Platikanov, L. Liggieri, R. Miller; CRC Press Published July 19, 2018; ISBN 9781466587724.
8. Drenckhan W, Saint-Jalmes A: *Adv. Colloid Interface Sci.* 2015, **222**:228.
9. Drenckhan W, Hutzler S: *Adv. Colloid Interface Sci.* 2015, **224**:1.
10. Saint-Jalmes A: *Soft Matter* 2006, **2**:836.
11. Rio E, Drenckhan W, Salonen A, Langevin D: *Adv. Colloid Interface Sci.* 2014, **205**:74.
12. Fameau AL, Salonen A, R C: *Physique* 2014, **15**:748.
13. Cohen-Addad S, Höhler R: *Curr. Opin. Colloid Interface Sci.* 2014, **19**:536.
14. Dollet B, Raufaste C, R C: *Physique* 2014, **15**:731.
15. Weaire D, Findlay S, Verbist G: *J. Phys. Condens. Matter* 1995, **7**:1217.
16. Feitosa K, Marze S, Saint-Jalmes A, Durian DJ: *J. Phys. Condens. Matter* 2005, **17**:6301.
17. Karapantsios TD, Papara M: *Colloids Surf. A* 2008, **323**:139.
18. Yazhgur P, Honorez C, Drenckhan W, Langevin D, Salonen A: *Phys. Rev. E* 2015, **91**, 042301.
19. Vera MU, Saint-Jalmes A, Durian DJ: *Appl. Opt.* 2001, **40**:4210.
20. Forel E, Rio E, Beguin S, Hutzler S, Weaire D, Drenckhan W: *Soft Matter* 2016, **12**:8025.
21. Cohen-Addad R Höhler S, Durian DJ: *Curr. Opin. Colloid Interface Sci.* 2014, **19**:242.
22. Meagher AJ, Mukherjee M, Weaire D, Hutzler S, Banhart J, Garcia-Moreno F: *Soft Matter* 2011, **7**:9881.
23. Raufaste C, Dollet B, Mader K, Santucci D, Mokso R: *EPL* 2015, **111**.
24. de Krasinski JS, Khosla A, Ramesh V: *Arch. Mech.* 1978, **30**:461–475.
25. Orenbakh ZM, Shushkov GA: *Sov. Phys. Acoust.* 1992, **38**:2.
26. Orenbakh ZM, Shushkov GA: *Acoust. Phys.* 1993, **39**:63.
27. Goldfarb I, Orenbach Z, Schreiber I, Vafina F: *Shock Waves* 1997, **7**:77.  
\*  
pioneering work
28. Moxon NT, Torrance AC, Richardson SB: *Appl. Acoust.* 1988, **24**:193.  
\*\*  
Important pioneering work
29. Zamashchikov VV, Kakutkina NA: *Sov. Phys. Acoust.* 1991, **37**:248.  
\*  
Important pioneering work
30. Shushkov G, Feklistov V: *Acoust. Phys.* 1995, **41**:283.
31. Mujica N, Fauve S: *Phys. Rev. E* 2002, **66**.  
first experimental data at high frequencies; clear evidence of an influence of **R**
32. Pierre J, Leroy V, Saint-Jalmes A, Dollet B, Ben Salem I, Crassous J, Guillermic R-M, Drenckhan W, Elias F: *Proc. Meet. Acoust.* 2013, **19**, 045044.
33. Pierre J, Guillermic R-M, Elias F, Drenckhan W, Leroy V: *Eur. Phys. J. E.* 2013, **36**:113.
34. Albert Beaumont Wood, *A Text Book of Sound* G. Bell and Sons, London, (1941).
35. Gardiner BS, Dlugogorski BZ, Jameson GJ, Chhabra RP: *J. Rheol.* 1998, **42**:1437.
36. Kann KB: *Colloids Surf. A* 2005, **263**:315.  
introducing important theoretical elements
37. Monloubou M, Saint-Jalmes A, Dollet B, Cantat I: *EPL* 2015, **112**:34001.
38. Pierre J, Gaulon C, Derec C, Elias F, Leroy V: *Eur. Phys. J. E* 2017, **40**:73.  
\*  
identifying and classifying the different mechanisms of dissipation in foams
39. Erpelding M, Guillermic R-M, Dollet B, Saint-Jalmes A, Crassous J: *Phys. Rev. E* 2010, **82**, 021409.
40. Ben Salem I, Guillermic R-M, Sample C, Leroy V, Saint-Jalmes A, Dollet B: *Soft Matter* 2013, **9**:1194.
41. Pierre J, Dollet B, Leroy V: *Phys. Rev. Lett.* 2014, **112**:148307.  
complete data set and model reconciling different discrepancies
42. Monloubou M, Bruning M, Saint-Jalmes A, Dollet B, Cantat I: *Soft Matter* 2016, **12**:8015.
43. Erpelding M, Guillermic R-M, Pierre J, Dollet B, Saint-Jalmes A, Crassous J: *Proc. Meet. Acoust.* 2013, **19**:45038.
44. Crassous J, Chasles P, Pierre J, Saint-Jalmes A, Dollet B: *Phys. Rev. E* 2016, **93**, 032611.  
\*  
an original setup to measure acoustic properties of foams by optical means

45. Wintzenrieth F, Cohen-Addad S, Le Merrer M, Höhler R: *Phys. Rev. E* 2014, **89**, 012308.
46. Afenchenko VO, Ezersky AB, Kiyashko SV, Rabinovich MI, Weidmann PD: *Phys. Fluids* 1998, **10**:390.
47. Boudaoud A, Couder Y, Ben Amar M: *Phys. Rev. Lett.* 1999, **82**:3847.
48. Besson S, Debregeas G: *Eur. Phys. J. E* 2007, **24**:109.
49. Faerman VT: *Acoust. Phys.* 2016, **62**:24.
50. Britan A, Liverts M, Ben-Dor G: *Colloids Surf. A* 2009, **344**:48.
51. Goldfarb II, Orenbakh ZM, Shushkov GA, Shreiber IR, Vafina FI: *J. Phys. IV* 1992, **2**:C1–C891.
52. Cohen A, Fraysse N, Raufaste C: *Phys. Rev. Lett.* 2017, **119**:238001.
53. Hutzler S, Saadatfar M, van der Net A, Weaire D, Cox SJ: *Colloids Surf. A* 2008, **323**:123.
54. Cohen A, Fraysse N, Rajchenbach J, Argentina M, Bouret Y, Raufaste C: *Phys. Rev. Lett.* 2014, **112**:218303.
55. Harazi M, Rupin M, Stephan O, Bossy E, Marmottant P: *Phys. Rev. Lett.* 2019, **123**:254501.
56. C. Y. Ng, H. Park, and L. Wang, *Langmuir* DOI: 10.1021-acs-langmuir-9b03767.
57. Pierre J, Giraudet B, Chasle P, Dollet B, Saint-Jalmes A: *Phys. Rev. E* 2015, **91**, 042311.
58. Kosgodagan Acharige S, Elias F, Derec C: *Soft Matter* 2014, **10**:8341.  
\*\* identifying the dominant role of viscous dissipation in the attenuation of a vibration wave on a soap film
59. Derec C, Leroy V, Kaurin D, Arbogast L, Gay C, Elias F: *EPL* 2015, **112**:34004.  
\* understanding the dynamics of Plateau borders under mechanical solicitations
60. Seiwert J, Pierre J, Dollet B: *J. Fluid Mech* 2016, **788**:183.
61. Lucassen J: *J. Colloid Interface Sci.* 1982, **85**:52.
62. Stenvot C, Langevin D: *Langmuir* 1988, **4**:1179.
63. Mariot S, Leroy V, Pierre J, Elias F, Bouthemy E, Langevin D, Drenckhan W: *Colloids Surf. A* 2015, **473**:11.
64. Elias F, Hutzler S, Ferreira MS: *Eur. J. Phys.* 2007, **28**:755.
65. Drenckhan W, Dollet B, Hutzler S, Elias F: *Philos. Mag. Lett.* 2008, **88**:669.
66. Elias F, Janiaud E, Bacri J-C, Andreotti B: *Phys. Fluids* 2014, **26**, 037101.
67. Elias F, Kosgodagan Acharige S, Rose L, Gay C, Leroy V, Derec C: *Colloids Surf. A* 2017, **534**:85.
68. Gaulon C, Derec C, Combriat T, Marmottant P, Elias F: *Eur. J. Phys.* 2017, **38**, 045804.
69. Couder Y, Chomaz JM, Rabaud M: *Physica D* 1989, **37**:384.
70. van der Meer SM, Dollet B, Voormolen MM, Chin CT, Bouakaz A, de Jong N, Versluis M, Lohse D: *J. Acoust. Soc. Am.* 2007, **121**:648.
71. Gaulon C, Pierre J, Leroy V, Elias F, Derec C: *Acta Acustica* 2018, **104**:193.
72. Gaulon C, Pierre J, Derec C, Jaouen L, Becot F-X, Chevillotte F, \* Elias F, Drenckhan W, Leroy V: *Appl. Phys. Lett.* 2018, **112**:261904.  
investigating the transition from liquid to solid foams
73. Nauber R, Büttner L, Eckert K, Fröhlich J, Czarske J, Heitkam S: *Phys. Rev. E* 2018, **87**, 013113.
74. Champougny L, Pierre J, Devulder A, Leroy V, Julien M-C: *Eur. Phys. J. E* 2019, **46**.
75. Leroy V, Strybulevych A, Lanoy M, Lemoult F, Tourin A, Page JH: *Phys. Rev. B* 2015, **91**, 020301.
76. Leroy V, Chastrette N, Thieury M, Lombard O, Tourin A: *Fluids* 2018, **3**:95.
77. Jin Y, Kumar R, Poncelet O, Mondain-Monval O, Brunet T: *Nat Commun* 2019, **10**:143.